第 33 卷第 10 期　　焊　接　学　报　　Vol. 33　No. 10
2012 年 10 月　　TRANSACTIONS OF THE CHINA WELDING INSTITUTION　　October　2012

时效温度对 15-5PH 沉淀硬化不锈钢熔敷金属组织和性能的影响

齐彦昌，　张晓牧，　彭　云，　田志凌*
（钢铁研究总院 先进钢铁流程及材料国家重点实验室，北京　100081）

齐彦昌

摘　要： 时效温度是 15-5PH 沉淀硬化不锈钢熔敷金属时效处理的重要参数，对组织和性能具有重要的影响. 采用钨极氩弧焊将研制的焊丝进行熔敷金属焊接试验，并将熔敷金属固溶处理后进行不同温度的时效处理，研究时效温度对熔敷金属组织和性能的影响. 结果表明，时效处理后熔敷金属组织主要为马氏体、残余奥氏体和 ε-Cu 析出相. 随着时效温度的增高，组织中奥氏体含量增多，尤其在 621 ℃时含量急剧增加；马氏体板条析出 ε-Cu 尺寸逐渐增大，而数量先增多后减少；另外随着时效温度的增高，熔敷金属强度下降，而冲击韧性升高，这主要是由于残余奥氏体含量增多引起的.

关键词： 时效温度；　组织；　性能；　熔敷金属
中图分类号： TG142.4　　**文献标识码：** A　　**文章编号：** 0253－360X(2012)10－0105－04

0　序　　言

15-5PH 钢是在 17-4PH 钢基础上，通过增加镍含量，降低铬含量进一步优化的马氏体析出硬化不锈钢，具有良好的横向韧性、延展性以及抗腐蚀能力. 其最主要的特点是经 480～620 ℃之间不同温度时效处理后，可以获得很宽的强度范围，并同时具有优良的塑、韧性. 特别适合于制造高强度、耐腐蚀的精密零件[1-3].

15-5PH 钢具有良好的焊接性，可以用作焊接结构钢. 而在国内与 15-5PH 钢配套焊接材料尚属空白，因而立项开发 15-5PH 钢配套的焊接材料，在国内尚属首次研制. 15-5PH 钢焊接接头经过不同时效工艺处理后，焊缝金属可以获得不同的强度与韧性. 因此，时效处理对焊缝金属的组织和性能具有很大的影响.

研究时效温度对 15-5PH 不锈钢焊丝熔敷金属组织和性能的影响，这为开发性能优异沉淀硬化不锈钢焊接材料提供重要理论基础.

1　试验方法

熔敷金属焊接采用钨极氩弧焊，试板单边坡口角度为 22.5°，间隙为 12 mm. 采用自制焊丝，焊丝熔敷金属的化学成分如表 1 所示. 焊丝直径为 1.6 mm. 焊接设备为艾美特钨极氩弧自动焊机，焊接电流为 240 A，电弧电压为 13 V，热输入为 15.6 kJ/cm. 焊接完毕，首先将 1 040 ℃固溶处理，而后分别将熔敷金属进行 482，496，552，593，621 ℃时效处理，空冷.

表 1　熔敷金属的化学成分（质量分数，%）
Table 1　Chemical compositions of welding deposite

C	Si	Mn	P	S	Cr	Ni	Cu	Fe
0.035	0.47	0.30	0.0057	0.005	14.86	5.18	3.30	余量

熔敷金属用砂纸研磨、抛光和腐蚀后，利用 LeicaMEF-4M 光学显微镜及 SCIAS6.0 图像分析系统观察熔敷金属的金相组织. 透射试样片用砂纸磨到 50 μm 以下，用 MTP-1A 磁力减薄器电解双喷减薄，减薄液为 6% 高氯酸乙醇溶液，温度为 －25 ℃，电压为 25 V，电流为 60 mA. 采用 H-800 透射电镜研究微观精细结构. 冲击试验温度为室温.

2　试验结果与讨论

2.1　时效温度对组织的影响

熔敷金属中含有大量 Cr，Ni 和 Cu 等合金元素，奥氏体的稳定性非常强，在连续冷却过程中，消除了

收稿日期：2011－08－30
* 参加此项研究工作的还有杨帅

高温和中温转变组织，其组织主要为马氏体. 经过不同温度的时效处理后，组织发生了变化.

经过 482 ℃或 552 ℃时效处理后熔敷金属金相组织主要为马氏体，如图 1a，b 所示. 而经过 621 ℃时效处理后组织除了马氏体外还含有较多的残余奥氏体，如图 1 所示. 图 1c 中板条间白色块状组织为奥氏体. 在透射下观察经过 621 ℃时效处理熔敷金属同样发现组织除了马氏体外还含有较多的奥氏体，如图 2 所示. 需要说明的是图 2b 暗场像中不仅显示了奥氏体相还将 ε-Cu 析出相显示出来(暗场中白色亮点)，这主要是由于奥氏体相和 ε-Cu 析出相都是面心立方，且点阵常数非常接近. 采用 EBSD (electron back scatter diffraction) 技术研究时效温度对残余奥氏体含量的影响，如图 3 所示. 图 3 中可以看出随着时效温度的升高残余奥氏体含量增加，并且在 621 ℃时残余奥氏体含量急剧增加. 文献[4]表明在 621 ℃进行时效温度处理时，由于此温度已进入奥氏体转变区域，马氏体直接转变成奥氏体，即逆转奥氏体. 在随后的冷却过程中大量的逆转奥氏体被保留下来.

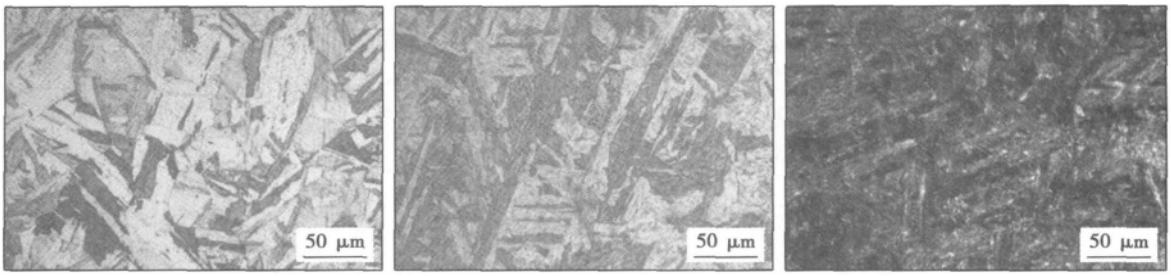

(a) 时效温度482 ℃ (b) 时效温度552 ℃ (c) 时效温度621 ℃

图 1 不同时效温度的金相组织

Fig. 1 Metallographic structures with different aging temperatures

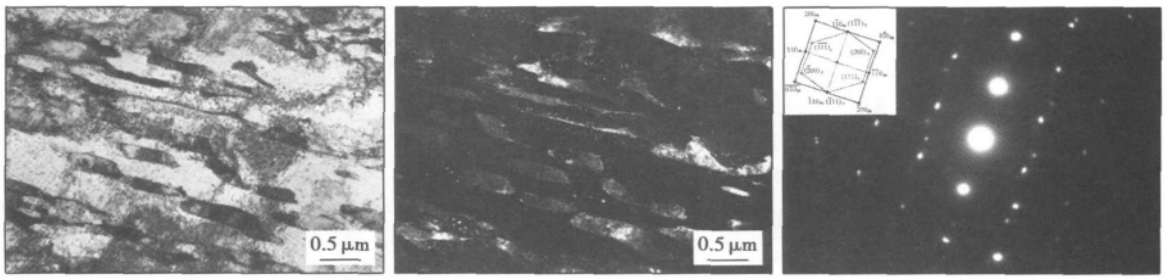

(a) 明场 (b) 暗场 (c) 马氏体和奥氏体相衍射花样

图 2 621 ℃时效后 TEM 组织

Fig. 2 TEM image after aging at 621 ℃

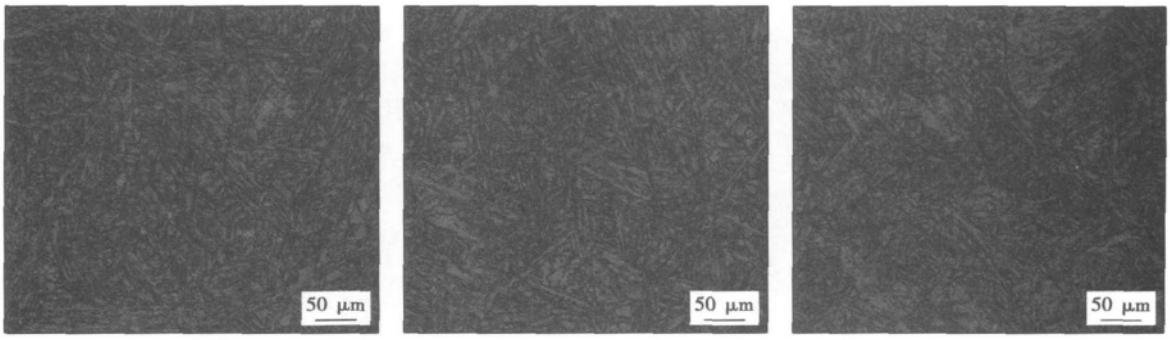

(a) 时效温度482 ℃ (b) 时效温度552 ℃ (c) 时效温度621 ℃

图 3 不同时效温度的奥氏体含量

Fig. 3 Austenite contents with different aging temperatures

熔敷金属中含有较多的铜，经过固溶处理后铜主要固溶在马氏体中，铜在马氏体中稳定性较差，经过时效处理后易以 ε-Cu 的形式从马氏体板条内析出，而 ε-Cu 析出相作为强化相存在[5,6]. 图 4 为熔敷金属中马氏体析出 ε-Cu 相. 研究发现随着时效温度的升高，ε-Cu 析出相尺寸增大，数量先增多后减少，这主要是在 621 ℃时效时析出相 ε-Cu 聚集长大造成的.

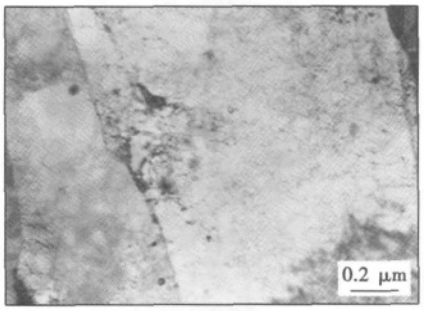

(a) 时效温度481 ℃

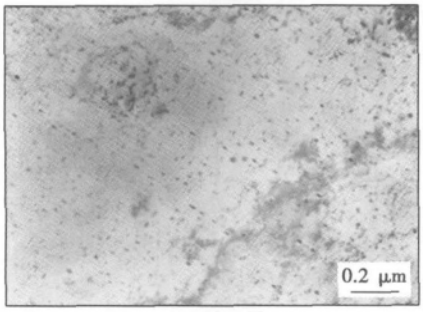

(b) 时效温度552 ℃

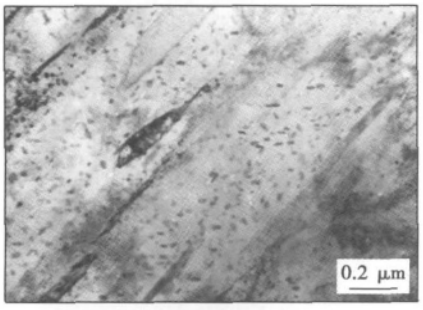

(c) 时效温度621 ℃

图 4　在不同时效温度时马氏体析出 ε-Cu

Fig. 4　ε-Cu precipitated in martensite with different aging temperatures

2.2　时效温度对力学性能的影响

时效温度对熔敷金属的强度有重要的影响，从图 5a 中可以看出随着时效温度的增大，抗拉强度均匀下降，而屈服强度也随之下降. 另外发现当时效温度大于 593 ℃后，屈服强度曲线斜率急剧变陡，经过前面的组织分析可知，这主要是由于经过 621 ℃时效后，组织中残余奥氏体含量较多. 随着时效温度的增大，熔敷金属的冲击韧性增加，如图 5b 所示，这主要也是韧相残余奥氏体含量增多引起，而 ε-Cu 作为强化相，它的聚集长大对韧性并无积极作用.

图 6 为冲击断口宏观形貌. 观察发现，482 ℃断口形貌由纤维区和晶状区组成，纤维率为 55%，而 552 ℃和 621 ℃时断口纤维率为 100%. 采用 SEM 观察 482 ℃冲击断口形貌发现，微裂纹首先在缺口处萌生，并且稳定扩展形成灰暗色的纤维状形貌，裂纹稳定扩展一定距离后裂纹发生失稳形成结晶状形貌. 纤维区发现分布大量韧窝，它们均以微孔聚集型方式断裂，如图 7a 所示. 韧窝内存在夹杂物，夹杂物的成分，如图 7b 所示. 晶状区以解理断裂和微

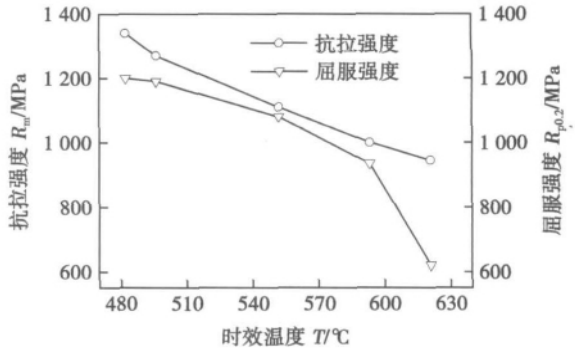

(a) 时效温度对强度的影响

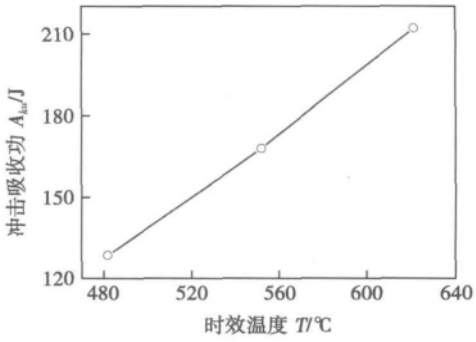

(b) 时效温度对室温韧性的影响

图 5　时效温度对力学性能的影响

Fig. 5　Effect of aging temperature on properties

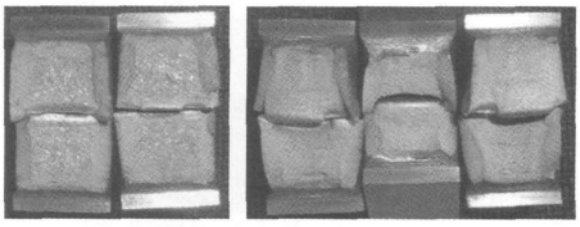

(a) 时效温度482 ℃　　(b) 时效温度552 ℃

图 6　冲击断口的宏观形貌

Fig. 6　Macroscopical morphology of impact fracture

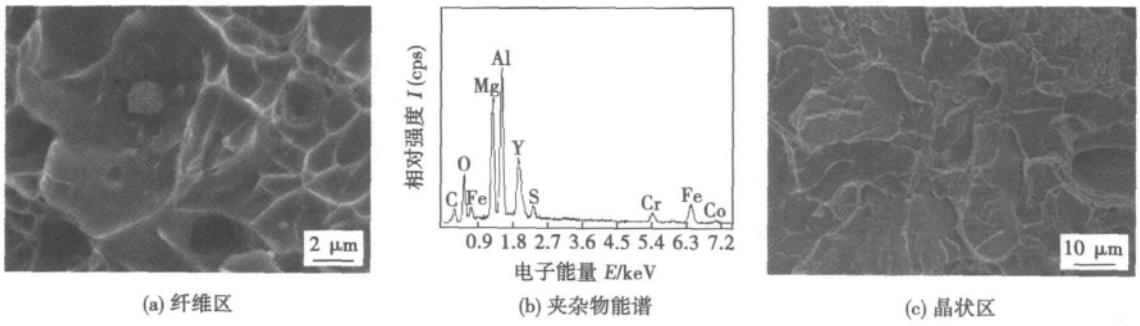

(a) 纤维区 (b) 夹杂物能谱 (c) 晶状区

图7 冲击断口微观形貌(482 ℃)

Fig. 7 Microscopical morphology of impact fracture

孔聚集型混合模式断裂,如图7c所示.

3 结 论

(1) 时效后熔敷金属组织主要为马氏体、残余奥氏体和析出相 ε-Cu.

(2) 随着时效温度的增高,组织中奥氏体含量增多,在温度达621 ℃时急剧增多.

(3) 随着时效温度的增高,马氏体板条析出 ε-Cu 尺寸逐渐增大,数量先增多后减少.

(4) 随着时效温度的增高,熔敷金属的强度下降,而冲击韧性升高,这主要是由于残余奥氏体含量增多引起的.

参考文献:

[1] Habibi B H R. The effect of ageing upon the microstructure and mechanical properties of type 15-5PH stainless steel [J]. Materials Science and Engineering A, 2002, 338: 142 - 159.

[2] 李 伟, 杜 楠, 樊兆宝. 15-5PH 马氏体时效钢的工艺性能 [J]. 兵器材料科学与工程, 2010, 33(1): 78 - 80.
Li Wei, Du Nan, Fan Zhaobao. Technological properties of 15-5PH maraging steel [J]. Ordnance Material Science and Engineering, 2010, 33(1): 78 - 80.

[3] 华小珍, 魏振伟, 刘智勇, 等. 固溶处理对 15-5PH 不锈钢马氏体相变的影响 [J]. 金属热处理, 2011, 36(8): 67 - 70.
Hua Xiaozhen, Wei Zhenwei, Liu Zhiyong, *et al*. Effect of solution treatment on martensitic transformation of 15-5PH stainless steel [J]. Heat Treatment of Metals, 2011, 36(8): 67 - 70.

[4] 刘振宝, 梁剑雄, 杨志勇, 等. 碳含量对 15-5PH 沉淀硬化不锈钢板材的组织与性能的影响 [J]. 航空材料学报, 2011, 31(1): 7 - 12.
Liu Zhenbao, Liang Jianxiong, Yang Zhiyong, *et al*. Effect of carbon content on microstructure and mechanical properties of type 15-5PH precipitation hardened stainless steel [J]. Journal of Aeronautical Materials, 2011, 31(1): 7 - 12.

[5] Aghaie K M, Adhami F. Hot deformation of 15-5 PH stainless steel [J]. Materials Science and Engineering A, 2010, 527: 1052 - 1057.

[6] Brooks J A, Garrison W M. Weld microstructure development and properties of precipitation strengthened martensitic stainless steels [J]. Welding Journal, 1999, 78(8): 280 - 291.

作者简介: 齐彦昌,男,1980年出生,博士. 主要从事焊接材料研发及焊接工艺性研究工作. 发表论文15余篇. Email: qiyanchang@163.com

creases. On the basis of differences in equivalent cathode/anode drops and the welding arc characters in EN/EP polarity, the welding wire gets more energy as the EN ratio increases, so the wire melting rate is larger than DC MIG welding. At a constant wire feed speed and welding speed, the penetration depth and bead width decrease while the reinforcement becomes high as the EN ratio increases. Accordingly, AC Pulse MIG welding technology can solve the burn through problem in welding thin sheet joints and can greatly improve the gap bridging ability in lap joints. What is more, this technology can also improve the welding speed and welding bead quality for thin sheet joints.

Key words: aluminum alloy welding; AC pulse MIG welding; EN ratio; wire welding rate

Analytical model of wire temperature distribution during hot-wire TIG welding process ZHAO Fuhai[1,2], HUA Xueming[1,2], YE Xin[1,2], WU Yixiong[1,2,3] (1. Welding Engineering Institute of Material Science and Engineering Shanghai Jiaotong University, Shanghai 200240, China; 2. Shanghai Key Laboratory of Materials Laser Processing and Modification, Shanghai Jiaotong University, Shanghai 200240, China; 3. State Key Laboratory of Metal Matrix Composite, Shanghai Jiaotong University, Shanghai 200240, China). pp 97 – 100

Abstract: Based on the law of energy conservation, the mathematical model considering the effect of heat loss on the hot-wire temperature distribution was developed. The accuracy of the mathematical model was validated by comparing the calculating result with the experimental results. The effect of wire diameter, hot-wire current, wire feeding speed, and wire extension on temperature distribution of hot-wire elaborately was discussed. The results show that the mathematical model has so high accuracy that it can be used to analyze the heating process of wire and satisfies the need of controlling the welding quality. The smaller the wire diameter and wire feeding speed are, the higher the temperature of the position on the wire extension having the same distance away from the power-feeding point is. The higher hot-wire current is, the higher the temperature is. However, the larger the wire extension is, the higher the temperature of the position on the wire having the same distance away from the wire-feeding point is.

Key words: hot-wire TIG welding process; heat-loss; temperature distribution of hot-wire; mathematical analytical model

Development of flux for Sn-Zn lead-free solder HAN Ruonan[1], XUE Songbai[1], HU Yuhua[2], WANG Zongyang[1], JA Jianyi[1] (1. College of Materials Science and Technology, Nanjing University of Aeronautics and Astronautics, Nanjing 210016, China; 2. The 55th Research Institute, China Electronic Technology Group Corporation, Nanjing 210016, China). pp 101 – 104

Abstract: The speadabitity of Sn-9Zn solder on Cu substrate with four different types of flux was studied by spreading experiment method. The experimental results indicated that Sn-9Zn solder, matching the flux-A4 with stannous sulfonate (20%) as the main activator without halogen which exhibited excellent wettability. The largest spreading area was 65.7 mm^2, increased respeetively by 16.1%, 116.1%, 85.1% compared with the NH_4Cl-$ZnCl_2$, resin and water-solubility fluxes. Besides, the newly developed flux with combination of 20% stannous sulfonate and diethanolamine, succinic acid could remarkably improve the wettabiltiy of Sn-9Zn solder that the largest spreading areas were 76.5 mm^2, 72.5 mm^2 when the contents of diethanolamine, succinic acid were at 8%, 10%.

Key words: Sn-Zn; soldering flux; spreading areas

Effect of aging temperature on microstructure and properties of deposited metal for type 15-5PH precipitation hardened stainless steel QI Yanchang, ZHANG Xiaomu, PENG Yun, TIAN Zhiling (State Key Laboratory of Advanced Steel Processes and Products, Central Iron & Steel Research Institute, Beijing 100081, China). pp 105 – 108

Abstract: Aging temperature is an important aging treatment parameter of deposited metal for type 15-5PH precipitation hardened stainless steel. The welding deposited metal was conducted by gas tungsten arc welding and aging treatment was carry out at different temperature after solution treatment. After aging treatment the microstructure and properties of deposited metal were investigated. The results indicate that microstructure of deposited metal by aging treatment consists predominately of martensite, residual austenite and ε-Cu. The increasing of aging temperature results in the increasing of amount of austenite and the size of ε-Cu, the variation of ε-Cu from increasing to decreasing. The strength of deposited metal drops and toughness improves with the increasing of aging temperature due to the increasing of amount of austenite.

Key words: aging temperature; microstructure; properties; deposited metal

Structure and mechanical properties of TC4/TC17 linear friction welding joint JI Yajuan[1], LIU Yanbing[2], ZHANG Tiancang[1], ZHANG Chuanchen[1] (1. AVIC Beijing Aeronautical Manufacturing Technology Research Institute, Beijing 100024, China; 2. No. 94170 Unit of People's Liberation Army, Xi'an 710061, China). pp 109 – 112

Abstract: TC4 and TC17 titanium usually used on aero-engine blisk were studied. The microstructures were analyzed by metallograph and transmission electron microscope. The temperature during the welding process was also measured. The investigation showed that the joints included three zones, base metal (BM), thermal mechanical affected zone (TMAZ) and welding zone(W). The TMAZ microstructure was similar to base metal, alpha and beta phase were elongated along the stress direction, recrystallization occurred in the weld zone. The induced microstructures were different from the BM. The maximum temperature can reach 1 270 ℃ which exceeds the titanium beta transformation temperature. the tensile test result showed that joint tensile strength was equal to that of the TC4 at room temperature and 200 ℃, while the testing temperature is 400 ℃, the joint tensile strength can reach 95% of the TC4 base mental.

Key words: linear friction welding; titanium; microstructure; temperature